Wood-Ljungdahl pathway utilisation during in situ H2 biomethanation

de Jonge, Nadieh; Poulsen, Jan Struckmann; Vechi, Nathalia Thygesen; Kofoed, Michael Vedel Wegener; Nielsen, Jeppe Lund

Published in:
Science of the Total Environment

DOI (link to publication from Publisher):
10.1016/j.scitotenv.2021.151254

Publication date:
2022

Document Version
Publisher's PDF, also known as Version of record

Science of the Total Environment 806 (2022) 151254

Contents lists available at ScienceDirect

Science of the Total Environment

journal homepage: www.elsevier.com/locate/scitotenv

Wood-Ljungdahl pathway utilisation during *in situ* H_2 biomethanation

Nadieh de Jonge [a], Jan Struckmann Poulsen [a], Nathalia Thygesen Vechi [b], Michael Vedel Wegener Kofoed [b], Jeppe Lund Nielsen [a,*]

[a] Department of Chemistry and Bioscience, Aalborg University, Fredrik Bajers Vej 7H, DK-9220 Aalborg E, Denmark
[b] Department of Biological and Chemical Engineering, Aarhus University, Hangøvej 2, DK-8200 Aarhus N, Denmark

HIGHLIGHTS

- Overall AD activity was maintained during *in situ* H_2 biomethanation.
- Protein-SIP was able to link microbial function and identity.
- Pre-adapted biomethanation showed the largest ^{13}C-bicarbonate incorporation.
- Pre-adapted biomethanation showed strong labelling of Wood-Ljungdahl pathway.
- Added H_2 was likely converted to acetate during pre-adapted biomethanation.

GRAPHICAL ABSTRACT

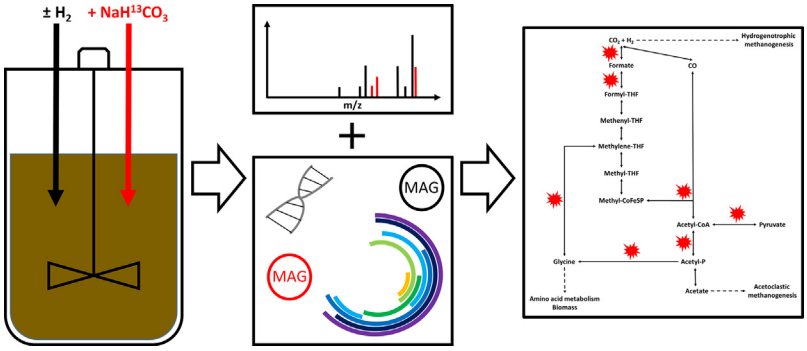

ARTICLE INFO

Article history:
Received 24 August 2021
Received in revised form 22 October 2021
Accepted 22 October 2021
Available online 26 October 2021

Editor: Qilin Wang

Keywords:
Protein-SIP
Anaerobic digestion
Biomethanation
Anaplerotic carbon fixation
Metagenomics
Wood-Ljungdahl pathway

ABSTRACT

Biogas production from organic waste is a waste-to-energy technology with the potential to contribute significantly to sustainable energy production. Upgrading of biogas using *in situ* biomethanation with hydrogen has the potential for surplus electricity storage, and delivery of biogas with a methane content of >90%, allowing for easier integration into the natural gas grid, as well as conversion to other products. Microbial communities in biomethanation reactors undergo changes, however, these changes are largely unexplored. In the present study, metagenome-resolved protein stable isotope probing (Protein-SIP) was applied to laboratory scale batch incubations operating under anaerobic digestion, and (pre-adapted) biomethanation conditions, fed with ^{13}C-labelled bicarbonate, in order to gain insight into the microbial activities during CO_2-reduction. The strongest and most microbially diverse isotopic incorporation was observed in the pre-adapted biomethanation incubation. Furthermore, divergent incorporation of ^{13}C-labelled bicarbonate was also observed in the Wood-Ljungdahl pathway, with the anaerobic digester incubations primarily showing labelled proteins in the peripheral pathways leading toward production of energy and biomass. The pre-adapted biomethanation incubations consumed H_2 and CO_2, but did not convert it to CH_4, suggesting the production of acetate in these incubations, which was supported by heavy labelling of key enzymes in the Wood-Ljungdahl pathway. Twelve (ten high quality) metagenome-assembled genomes (MAGs) coding for ^{13}C-incorporated proteins were extracted from the metagenome, eight of which contained one or more of the key genes in the Wood-Ljungdahl pathway, one of which was affiliated to *Methanosarcina*. Together, the findings in the present study deepen our knowledge surrounding microbial communities in biomethanation systems, and contribute to the development of better strategies for implementation of biogas upgrading and microbial management.

* Corresponding author.
E-mail addresses: ndj@bio.aau.dk (N. de Jonge), jsp@bio.aau.dk (J.S. Poulsen), navei@env.dtu.dk (N.T. Vechi), mvk@bce.au.dk (M.V.W. Kofoed), jln@bio.aau.dk (J.L. Nielsen).

https://doi.org/10.1016/j.scitotenv.2021.151254

1. Introduction

Anaerobic digestion (AD) is a renewable waste-to-energy technology that is based on the microbial conversion of organic biomass to methane-rich biogas. Biogas consists of a mixture of 55–80% methane (CH_4) and 20–45% carbon dioxide (CO_2) (Nizami, 2012), and is generally burned to generate heat and electricity, or upgraded to methane levels above 90%, while the digestate can be used as fertiliser or for the extraction of other valuable materials (Sawatdeenarunat et al., 2016).

In order to utilise biogas for other purposes than combined heat and power (CHP) generation, upgrading of the produced gas is often needed to remove contaminants and increase the methane content, partially due to quality requirements in *e.g.* natural gas grid (Angelidaki et al., 2018). Upgraded biogas contains a high methane content (≥90%; biomethane), can be stored and transported in the gas grid, wherefrom it can used for different industrial purposes (Graf et al., 2011). Hydrogen (H_2) addition to convert a portion of the produced CO_2 in the biogas to additional methane through the process of biomethanation represents a promising technology for upgrading the biogas to natural gas quality while valorising the CO_2 in the biogas (Angelidaki et al., 2018; Luo et al., 2012). Furthermore, biomethanation of hydrogen in anaerobic digesters has been proposed as a promising technology for the large-scale conversion and storage of electricity, from fluctuating sources such as wind and solar (Luo et al., 2012). However, due to limited knowledge regarding operation and the microbiome of such systems, only few studies have attempted to implement this technology in pilot- or even full-scale (Jensen et al., 2021).

Anaerobic digestion for the production of biogas is driven by a complex microbial community that reduces complex organic matter into monomeric substances (hydrolysis), followed by the production of volatile fatty acids (VFA) (acidogenesis) and hydrogen (H_2), which are subsequently converted to methane directly (methanogenesis) or to acetate (acetogenesis), which serves as substrate for acetoclastic methanogenesis (Weiland, 2010). The microbes involved in these processes become increasingly specialised as the pathway progresses, which is also reflected in their relative presence within the system. The AD process is regulated through a series of operational and physico-chemical parameters and kinetics, which control the activity of various pathways and interplays as well as the population dynamics (Carballa et al., 2015). Some of the most influential parameters that can radically alter the microbial community of a digester system are substrate composition, temperature, pH, H_2 partial pressure, VFA concentration and ammonia concentration (de Jonge et al., 2020; De Vrieze et al., 2015; Ward et al., 2008). The exact pH value at which CH_4 production rates start to decrease has been found to fluctuate in the range of pH 8.2–pH 8.5, and in one study as high as pH 9.4 (Agneessens et al., 2017; Luo et al., 2012; Wahid et al., 2019). Effects of H_2 partial pressure on the AD process have also yielded varying results, with one study reporting inhibition above an H_2 partial pressure of 745 mbar, while another reported no limitations at all (Lecker et al., 2017). Furthermore, previous studies have shown that biomethanation is dependent on the microbial community composition, and that the acetate consumption/production rates are strongly affected by the H_2 amendment (Agneessens et al., 2017; Vechi et al., 2021).

Key populations often linked to the stability and performance of an AD system include acetogens and methanogens, which live in close syntrophic relationships with each other (Narihiro et al., 2015). Syntrophic acetate oxidising organisms (SAO) convert acetate to CO_2 and H_2 using the Wood-Ljungdahl pathway, but are also able to reverse this pathway to generate acetate from CO_2 and H_2 (Hattori, 2008). This bi-directional conversion of acetate, CO_2 and H_2 allow swift changes between the acetoclastic (utilises acetate) and hydrogenotrophic (utilises CO_2 and H_2) methanogenesis pathways for methane production under different conditions, including stress (de Jonge et al., 2017; Fotidis et al., 2013). H_2 injection into the AD reactor with the purpose of supplying additional reducing equivalents for fuelling additional CH_4 formation likely will impact the delicate balances present in the AD system. This has also previously been suggested by a study focused on metagenomics analysis of the microbiome in biomethanation reactors (Treu et al., 2018).

In theory, the higher H_2 pressure in the reactor during H_2 addition should inhibit SAO (Hattori, 2008), and stimulate hydrogenotrophic methanogens, however *in situ* H_2 biomethanation in AD systems has generated conflicting reports; some studies have reported increased acetoclastic methanogenesis due to increased acetate production (homoacetogenesis) (Wang et al., 2013), while others have observed increased methanogenesis through the hydrogenotrophic pathway (Agneessens et al., 2017; Luo et al., 2012). Additional studies have also reported inhibition of (acetoclastic) methanogenesis (Ahring et al., 1991; Vechi et al., 2021), and acetate or general VFA accumulation due to the increased H_2 pressure (Corbellini et al., 2018; Mulat et al., 2017; Vechi et al., 2021), decreasing methane production in all cases. Hydrogen biomethanation for upgrading biogas presents a promising technology, but many open questions regarding the metabolic response of the digester microbiome remain. Targeted functional studies are needed to elucidate the metabolic pathway activity during anaerobic digestion with and without H_2 addition.

The majority of recent studies focusing on digester microbiomes have been based on metagenomic approaches such as 16S rRNA gene amplicon sequencing or shotgun metagenomics (Carabeo-Pérez et al., 2019). While these studies generate a wealth of information on the presence of microorganisms, they provide little information on the function or activity of specific microbes (Vanwonterghem et al., 2014). Protein stable isotope probing (protein-SIP) is a methodology where target communities are subjected to controlled incubations with stable isotope (*e.g.* ^{13}C, ^{15}N) labelled compounds in order to track uptake and incorporation of the isotopes into the proteome (*e.g.* Jehmlich et al., 2010). This approach has primarily been used in low diversity environments such as *in situ* microcosms for the study of polycyclic aromatic hydrocarbon degradation (Herbst et al., 2013), due to the limitations on protein identifications especially in complex ecosystems. In order to overcome the limitation of applying the protein-SIP approach in more complex environments, a methodology was developed where the protein-SIP data was combined with shotgun metagenomics, which allowed for the proteome data to be mapped to a metagenome of a digester system under VFA (acetate) stress, revealing new candidate SAO organisms by simultaneously linking identity and function (Mosbaek et al., 2016). A similar approach has also been applied to investigate the carbon flow in the rhizosphere microbiome of several model plants (Li et al., 2019).

The aim of the present study was to investigate differences in the metabolic behaviour of the microbial community during *in situ* H_2 biomethanation using metagenome-resolved protein stable isotope probing. Protein expression was studied in digester samples incubated with ^{13}C-labelled bicarbonate over a period of 48 h. Specific focus was on the detection of active CO_2-fixating microorganisms to evaluate the impact of H_2 addition on important anaerobic digestion processes such as syntrophic acetate oxidation, homoacetogenesis, and methanogenesis.

2. Materials and methods

2.1. Source of inoculum

Digester sludge was collected from a digester at the Maabjerg Energy Center biogas plant (Denmark), which processes primarily manures and dairy waste. This digester is operated under mesophilic conditions (40 °C) and has a hydraulic retention time of 18 days and produces approx. 50 million m^3 biogas annually (2020). The collected sludge was sieved up to 0.45 mm and subsequently transferred to the laboratory scale reactors (Section 2.2) or stored at −20 °C for later use as substrate.

2.2. Stable isotope probing

Six laboratory scale digesters were operated under mesophilic (38 °C) anaerobic CSTR conditions with a working volume of 0.3 L and a total volume of 1.4 L, stirred at 500 rpm. Reactors were fed using frozen slurry from the biogas digester where the inoculum was collected, as well as 1% (v/v) glycerol, which was fed semi-continuously as 9 pulses per day using a peristaltic pump. Glycerol was added to the substrate to boost the biogas production in the reactors (Fountoulakis et al., 2010). Three reactors received exogenous H_2 addition to induce H_2 biomethanation conditions, while the three other reactors without H_2 addition functioned as controls (anaerobic digestion). H_2 was added as four pulses of 379–424 mL H_2 per injection over a period of seven days, where 39–53% of the H_2 was consumed before H_2 was injected again. Prior to the addition of H_2, the biogas production in the control reactors and the H_2-receiving reactors was 0.37 L biogas·L digestate^{-1}·day^{-1} and 0.31 biogas·L digestate^{-1}·day^{-1}, respectively. The addition of H_2 increased the biogas production up to 1.59 biogas·L digestate^{-1}·day^{-1}.

After 30 days of operation, 120 mL of sludge was removed from the donor reactors and transferred to 250 mL serum flasks, and then flushed with N_2 for 5 min to achieve anaerobic conditions and flush CO_2 from the sludge. Subsequently, 2 g $NaH^{13}CO_3$ (final concentration 6.4 mmol·L^{-1} at pH 8.0) was added to each sample, and the pH was adjusted to 8.0 with 1 M HCl. Subsamples of 15 mL were taken from the isotopic incubations and transferred anaerobically to 0.12 L serum bottles, together with 1.5 mL substrate (sludge mixed with 0.5% glycerol). The bottles were divided into three treatments: Anaerobic digestion conditions, unadapted H_2 biomethanation conditions and pre-adapted H_2 biomethanation conditions. A total of 34 mL of H_2 was added to the (un)adapted biomethanation incubations to achieve the desired headspace composition. All three treatments were performed in triplicates. The headspace composition at the start of the isotopic incubation was 96:4% N_2:CO_2 and 55:41:4% N_2:H_2:CO_2 in the anaerobic digestion and H_2-receiving flasks, respectively. Samples were collected from each flask at the start (T0) and after 48 h (T48) of the experiment, and immediately transferred to, and stored at −18 °C until further processing.

2.3. Analytical methods

The headspace composition of the reactors (H_2, CO_2 and CH_4) was analysed periodically by direct-injection of the gas samples into a GC-TCD (Pora-Pak Q column, Mikrolab A/S), operated at 40 °C using argon as the carrier gas, with continuous monitoring by pressure sensors (MPX4250, NXP Semiconductors) attached to the bottles. pH was determined at the start (T0) and end of the experiment (T48).

2.4. Metaproteomics

For each treatment, three samples from the individual reactors, as well as a pooled sample from all 3 bottles per treatment, for a total of 4 samples per treatment, were collected for metaproteomic analysis of all time points and treatments. Protein extraction, in-solution digestion and desalting were performed as described elsewhere (Peydaei et al., 2020) on 700 μL of slurry per replicate.

Liquid chromatography-tandem mass spectrometry was performed using an Easy nLC 1200 system (Thermo Fisher Scientific) coupled to a Q-Exactive HF mass spectrometer equipped with a Nanospray Flex ion source. Peptides were injected into an Acclaim PepMap™ 100 (100 μm × 2 cm, NanoViper, C18, 5 μm, 100 Å) (Thermo Fisher Scientific) trap column and separated on an analytical column (PepmapRSLC, C18, 75 μm i.d. × 75 cm, 100 Å, Thermo Fisher Scientific). Samples were eluted at a flow rate of 300 nL·min^{-1} over a 60 min linear gradient, ranging from 0 to 100% acetonitrile as the mobile phase.

Mass spectrometry was performed, fragmenting precursors with an assigned charge of ≥2. An isolation window of 1.2 *m/z* was used, and survey scans were acquired at 400–1,200 *m/z* at resolution 60,000 at *m/z* 200, and fragmentation spectra were captured at 15,000 at *m/z* 200. Maximum ion injection time was set to 50 ms for MS and 45 ms for MS/MS scans. Automatic gain for survey scans was set to 1e6 ions and 1e5 ions for fragmentation scans. The apex trigger was not set, the intensity threshold was set to 4.4e4 ions, and dynamic exclusion of 30 s was applied. Normalized Collision Energy was set to 28, "peptide match" was set to "preferred", and "exclude isotopes" was enabled.

2.5. Metagenome preparation

A metagenome was generated from the biogas digesters at the Maabjerg Bioenergy plant. The metagenome was composed of 9 samples collected at different time points and reactors (Table S1). Different DNA extraction methods to increase diversity of the genomic information captured. A description of the samples and DNA extraction methods is listed in the Supplementary method. Genomic DNA concentrations were measured using dsDNA Broad Range Assay kit and a Qubit 3.0 fluorimeter (Thermo Fisher Scientific). Metagenomes were prepared using TruSeq DNA PCR-free Library Prep kit (Illumina) with a target insert size of 550 bp and 1 μg template DNA, according to manufacturer's recommendations. Sequencing was performed using an Illumina MiSeq platform using reagent kit v3 (2x300PE) (Illumina).

2.6. Data analysis

The individual metagenomes were processed into an assembly and coverage profiles were generated using CLC genomics workbench as previously described (Mosbaek et al., 2016). The metagenome was annotated using prokka version 1.14 (Seemann, 2014) using default settings.

The proteomics data was analysed using OpenMS (https://www.openms.de) and the MetaProSIP tool (Sachsenberg et al., 2015). The annotated protein sequences from the processed metagenomic assembly were used as the database to identify the peptides. Basic functional annotation of the identified proteins was assigned using the KEGG database (https://www.genome.jp/kegg/).

Data visualisation was performed using R version 3.5.2 (R Development Core Team, 2021) wrapped by RStudio version 1.1.463 (https://www.rstudio.com), using the packages ggplot2 (Wickham, 2016) and mmgenome2 (https://github.com/KasperSkytte/mmgenome2) (Albertsen et al., 2013). To facilitate analysis with mmgenome2, essential genes were identified in the metagenome using HMMER3 (http://hmmer.org/) against a list of 107 conserved single copy marker genes (Dupont et al., 2012), and basic taxonomy was assigned to the metagenome scaffolds using Kaiju (Menzel et al., 2016). The additional data was generated in accordance with the recommended data treatment for mmgenome2 (https://github.com/Kirk3gaard/misc_scripts/tree/master/prepare_data_for_mmgenome2).

Metagenome-assembled genomes (MAG) containing target genes for labelled peptides were extracted with the locator tool in mmgenome2 and checked for completeness and contamination using CheckM (Parks et al., 2015). Essential genes were identified in the bins using hmmsearch in HMMER3 and all hits with an E-value of 1e^{-50} or lower were identified using blastp, in order to taxonomically classify the bins to the highest taxonomic resolution possible. HMMER3 was also used to identify the presence of characteristic genes of the Wood-Ljungdahl (WL) pathway in the labelled bins. The HMMs used for screening are listed in Table S2.

2.7. Data availability

The combined raw metagenome data has been made available at the European Nucleotide Archive (ENA) under project accession number PRJEB46763, and the raw proteomic dataset has been deposited into ProteomeXchange *via* PRIDE under accession number PXD027519.

3. Results

3.1. ^{13}C-bicarbonate incubations

The ^{13}C-labelled bicarbonate incubations were performed in triplicates for each treatment, and the overall performance was determined from methane production rate, hydrogen consumption rate and composition of CO_2 in the headspace (Fig. 1). The unadapted biomethanation incubations were shown to have the highest methane production rate with 1.82 L $CH_4 \cdot L_{sludge}^{-1} \cdot day^{-1}$ at T48 (Fig. 1a) while the lowest methane production rate was observed in the pre-adapted biomethanation reactor, with 0.39 L $CH_4 \cdot L_{sludge}^{-1} \cdot day^{-1}$ at T48, which was similar to that of the anaerobic digestion flasks. The added hydrogen in the unadapted biomethanation and pre-adapted biomethanation incubations was largely consumed after 48 h of incubation, but a higher consumption rate of H_2 was observed in the unadapted biomethanation incubations during the first 8 h. The greatest differential increase in CH_4 production and H_2 consumption between replicates of the same treatment was seen in the unadapted biomethanation flasks, and the difference appeared to increase over the course of experiment. The proportion of CO_2 present in the headspace of the incubations increased steadily from around 6.5 to 10.5% in the anaerobic digestion bottles, while the unadapted biomethanation and pre-adapted biomethanation showed a stable amount of headspace CO_2 during the first 24 h of incubation, whereafter a decrease in CO_2 composition was observed in the pre-adapted biomethanation bottles. All reactors maintained very similar pH development during the entire experiment, not fluctuating more than 0.25 pH units between treatments, with a final pH of 8.56 ± 0.02, 8.74 ± 0.005 and 8.79 ± 0.01 in the anaerobic digestion, unadapted biomethanation and pre-adapted biomethanation incubations, respectively.

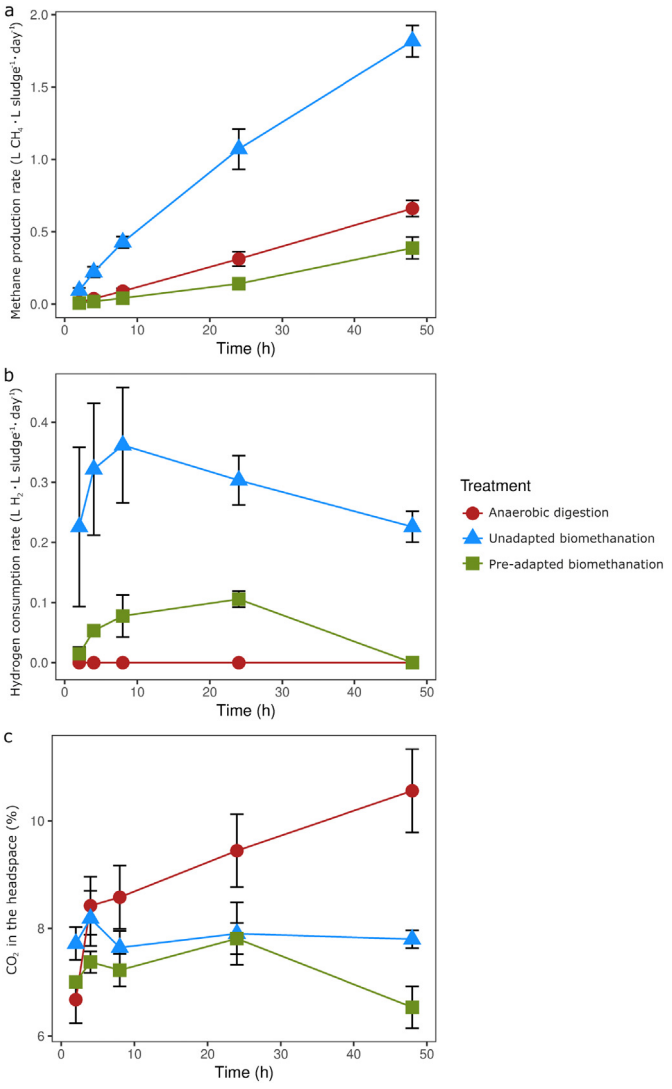

Fig. 1. Operational data. Methane production rate (a), hydrogen consumption rate (b) and CO_2 in the headspace (%) were monitored across 48 h of incubation.

3.2. Protein-SIP results

Protein-SIP analysis of the incubations generated a grand total of 793,855 peptides across all samples. Overall, 12,155 peptides (1.53%) were found to have assimilated labelled carbon in the three incubations. Stringent filtering with the conditions that peptides could not be labelled at T0, the peptide should be identified in at least 3 out of 4 replications from the analysed reactor, the amount of atoms replaced by their heavy isotopes (defined as the RIA) should be equal to or higher than 10, yielding a total of 91 labelled peptides of interest (Table S3). The anaerobic digestion, unadapted biomethanation and pre-adapted biomethanation samples contained 13, 9, and 69 peptides that were labelled in at least 3 of 4 replicates, respectively (Fig. 2). The identified labelled peptides in the anaerobic digestion and unadapted biomethanation incubations showed a low RIA (≤20), and a low labelling ratio (LR), although the anaerobic digestion samples revealed 5 peptides with a high LR (≥50%). The identified peptides in pre-adapted biomethanation bottles consisted of a large group with low LR and RIA, and two smaller groups of low RIA and high LR, and a high RIA (≥30) and LR, respectively. A general functional category was assigned to the labelled proteins using the KEGG database. This revealed the largest group of peptides (17) to be related to genetic information processing, followed by proteins associated with carbohydrate metabolism (14) and transport (12). A total of 28 uncharacterized proteins were also detected.

The majority of the labelled peptides belonged to organisms representing the phylum *Firmicutes* (Fig. 3), while smaller numbers of labelled peptides were associated to the phyla *Bacteroidetes*, *Proteobacteria*, *Euryarchaeota*, *Planctomycetes* and *Actinobacteria*, as well as some that were unclassified. *Firmicutes* and *Proteobacteria* represented the most labelled proteins in the anaerobic digestion reactors (Fig. 3a), while *Firmicutes*, *Bacteroidetes*, *Euryarchaeota* and *Actinobacteria* associated peptides were found to be labelled in the unadapted biomethanation reactors (Fig. 3b). The greatest diversity of labelling was seen in the pre-adapted biomethanation incubations, where the observed labelled peptides represented 7 different phyla (Fig. 3c), while only 4 and 3 phyla were observed in anaerobic digestion and unadapted biomethanation samples, respectively.

Peptides with the highest labelling ratio included representatives of Cold shock protein CspA and Transcriptional regulatory protein DegU (anaerobic digestion, *Firmicutes*), Propanediol utilisation protein PduA1 (unadapted biomethanation and pre-adapted biomethanation, *Firmicutes*), Membrane-bound lytic murein transglycosylase D (pre-adapted biomethanation, *Bacteroidetes*) and Amidophosphoribosyltransferase (pre-adapted biomethanation, *Euryarchaeota*, closely related to a representative of *Methanosarcina*). Some of the most heavily labelled peptides included Outer membrane protein alpha, Exoglucanase B (pre-adapted biomethanation, *Firmicutes*) and Peptide chain release factor 3 (pre-adapted biomethanation, *Bacteroidetes*). Many labelled peptides were found for proteins such as Flagellin FlaB2 (14 unique accessions), Elongation factor Tu (20 unique accessions) and 2 unclassified peptides related to Propanediol utilisation protein PduA (25 unique accessions total). Among peptides with lower isotope incorporation (RIA < 20), two different peptides representing ABC transporter ATP-binding protein NatA were observed from the unadapted biomethanation and pre-

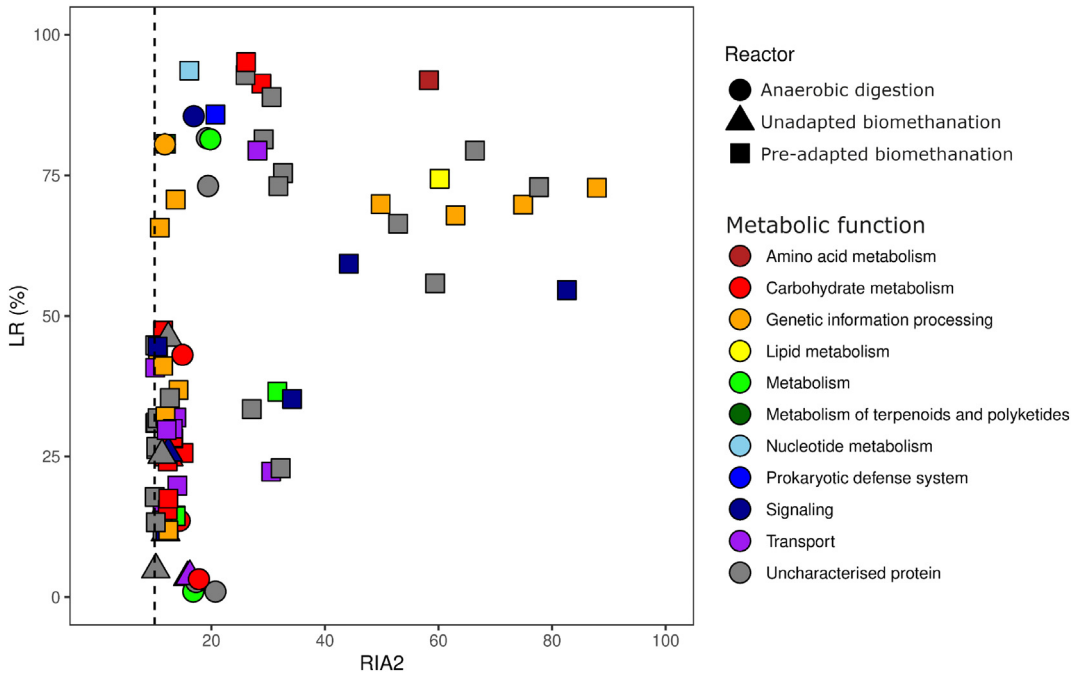

Fig. 2. Overview of peptides found in a higher labelling state. The relative incorporation abundance of peptides found to be in a higher labelling state (RIA) is shown against the observed labelling ratio (LR). Points are shaped by reactor of origin and coloured by the overall functional category of the identified peptides as identified by the KEGG database.

adapted biomethanation bottles, respectively, both of which were most closely related to a representative of *Methanothrix* (*Euryarchaeota*).

3.3. Extraction of labelled metagenome-assembled genomes

A total of 9 shallow metagenomes of Maabjerg Energy Center biogas digesters were sequenced (Table S1), which yielded a grand total of 90,291,334 paired-end reads, that when assembled yielded 942,321,460 bp. Three coverage profiles were generated based on the method of metagenome preparation (Table S1) and used to perform differential coverage binning (Fig. 4). The combined metagenome assembly consisted of 97.1% *Bacteria* and 2.9% *Archaea*, divided across a total of 37 different phyla, with *Firmicutes* being the most abundant representative with 62.3% of all identified scaffolds. A total of twelve MAGs (bin1–12), containing coding sequences for the labelled peptides, were extracted using differential coverage binning of the combined assembly against the three coverage profiles (Fig. 4). Two of the bins (bin1 and bin12) contained labelled peptides from the unadapted biomethanation incubations, while all others originated from the pre-adapted biomethanation bottles. In addition, two bins (bin7 and bin 11) contained labelled peptides from both the anaerobic digestion and pre-adapted biomethanation incubations. Quality control of the bins showed that bin1 had the highest quality with 99.43% completeness and 0.43% contamination, while bin5 had the lowest quality with 52.28% completeness and 0.17% contamination. Bin8 appeared to consist of two separate genomes. In total, five bins were of near complete quality, five were of substantial completeness, one was of moderate quality, and one was of low quality. All bins except bin8 contained low or no detectable contaminations.

Four of the twelve extracted bins (bin7, bin8, bin11 and bin12) were classified to the phylum *Firmicutes* and included representatives of *Clostridiales* and *Clostridiaceae* (Table 1). These bins contained between 1 and 5 labelled peptides each, including glycine cleavage system H protein and arginine-binding extracellular protein ArtP (Table S3), and all 4 bins also contained at least 1 of the key genes in the WL pathway. The *Euryarchaeota* bin (bin6) was classified to a representative of *Methanosarcina* and contained two labelled peptides. Three of four key proteins of the WL pathway were also identified in this bin. Another three bins were classified to *Bacteroidetes* (bin2, bin3) of which one belonged to *Marinilabiliales* (bin11), two *Actinobacteria* bins which were representatives of *Actinomycetaceae* (bin1), and *Propionibacteriaceae* (bin5). Finally, one bin represented *Candidatus* Cloacimonetes (bin9) and *Rhodobacteraceae* (*Proteobacteria*, bin4), respectively. All of these bins contained one labelled peptide each, including dihydroxy-acid dehydratase (bin1) and a putative sulfate transporter (bin5). Two key proteins of the WL pathway were also identified in the *Rhodobacteraceae* representative (bin4), as well as one WL key protein (formate tetrahydrofolate synthase) in bin2, bin3 and bin9.

3.4. Differential utilisation of the Wood-Ljungdahl pathway during anaerobic digestion and H_2 biomethanation

Addition of exogenous H_2 to anaerobic digesters is generally associated to activity in the Wood-Ljungdahl pathway, and labelling was also observed in a number of proteins associated with this pathway in the present study. The uptake and potential downstream utilisation of the labelled bicarbonate and CO_2 through this pathway was therefore examined in more detail. For this analysis, all observed labelled peptides were included ($n = 430$), even if they were observed in less than 3 out of 4 replications of a given incubation type. A full list of all labelled peptides is given in Table S4. The detection of labelled peptides in the Wood-Ljungdahl pathway and potential downstream metabolisms is visualised in Fig. 5.

All three reactors contained labelled peptides in the glycine cleavage system and glycine reductase complex, which are responsible for metabolism related to glycine formation and conversion with either methylene tetrahydrofolate from the methyl branch, and acetyl phosphate from the carbonyl branch of the Wood-Ljungdahl pathway, respectively. Glycine is a precursor for the production of other amino acids and potentially biomass. In the pre-adapted biomethanation incubations, the bifunctional carbon monooxide dehydrogenase/acetyl-CoA synthase enzyme was labelled, as well as phosphate acetyltransferase, and the formate-tetrahydrofolate ligase and formate dehydrogenase from the methyl branch of the WL pathway. Furthermore, a component

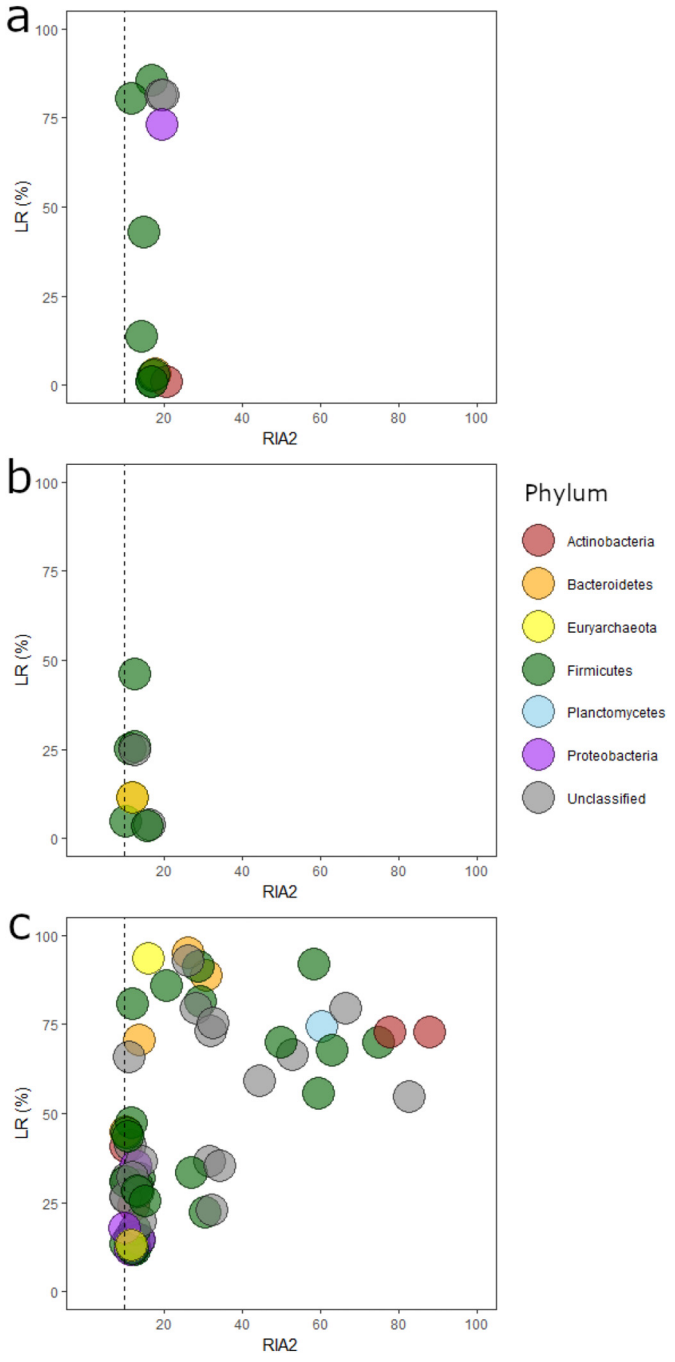

Fig. 3. Relative isotope abundance and labelling ratio of peptides in the anaerobic digestion (a), unadapted biomethanation (b) and pre-adapted biomethanation (c) incubations. Each peptide is coloured by taxonomic classification to phylum level.

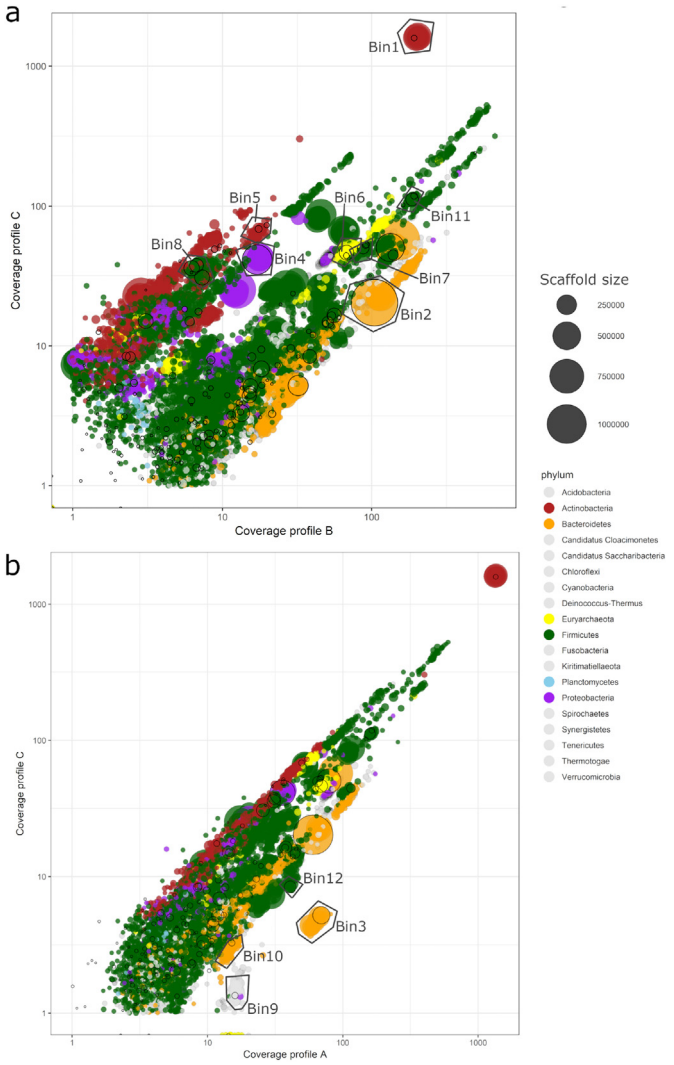

Fig. 4. Differential coverage binning of the combined metagenome, shown as coverage profiles B and C (a) and A and C (b), respectively. Dot size displays the scaffold length, only scaffolds longer than 10 kbp are shown. The 6 most abundant phyla are coloured, other taxonomic groups are shown in grey. Labelled scaffolds are shown with a black edge. Extracted bins are indicated with a polygon and the respective bin name.

of the pyruvate dehydrogenase complex (catalysing the bidirectional conversion between Acetyl-CoA and pyruvate) was isotopically enriched with ^{13}C in this incubation type.

4. Discussion

The aim of the present study was to investigate the metabolic differences in anaerobic digesters operating with and without hydrogen addition (biomethanation) using protein-SIP. After 48-hour incubations with ^{13}C-labelled bicarbonate, ^{13}C-labelled peptides were extracted from the proteome and mapped to a metagenome of the full-scale digester where the sludge was collected in order to identify active microorganisms during anaerobic digestion and biomethanation conditions.

4.1. Operational data for ^{13}C-bicarbonate incubations

At the end of the 48 hour incubation, the pH in all reactors was slightly higher (pH 8.5–8.8) compared to the pH at the start of the experiment (approximately pH 8.0). Continuous hydrogen addition to anaerobic digesters for *in situ* biomethanation has previously been shown to cause pH increases, due to increased CO_2 consumption and thus depletion of the major pH-buffering system (Agneessens et al., 2017). Increased pH could potentially also lead to more favourable conditions for homoacetogenesis, to the detriment of hydrogenotrophic methanogenesis (Saady, 2013). Uptake of H_2 increased in both receiving incubations during the first 10 h of the incubation, and then declined over time. This could potentially be explained by CO_2 depletion; a previous study has shown that headspace CO_2 below 12% resulted in decreased CH_4 production and increased pH due to its

Table 1
Detailed information on the twelve labelled MAGs.

Bin name	Treatment of origin	Scaffolds	Length (bp)	N50	GC content (%)	Identity	Completeness (%)	Contamination (%)	Labelled peptides	Number of uniquely identified essential genes	Wood-Ljungdahl biomarkers (x of 4)
Bin1	Unadapted biomethanation	20	2,033,697	197,329	53.35	*Actinomycetaceae* sp.	99.43	0.43	1	102	0
Bin2	Pre-adapted biomethanation	17	2,438,945	434,844	36.19	*Bacteroidetes* sp.	95.16	0.81	1	102	1
Bin3	Pre-adapted biomethanation	35	2,699,717	102,715	37.66	*Bacteroidetes* sp.	94.89	0.54	1	104	1
Bin4	Pre-adapted biomethanation	49	4,400,493	127,987	69.33	*Rhodobacteraceae* sp.	96.80	0.40	1	102	2
Bin5	Pre-adapted biomethanation	157	2,062,306	17,944	70.33	*Propionibacteriaceae* sp.	52.28	0.17	1	60	1
Bin6	Pre-adapted biomethanation	70	2,886,768	91,703	41.51	*Methanosarcina* sp.	95.71	1.96	2	29	3
Bin7	Anaerobic digestion/Pre-adapted biomethanation	107	1,499,749	28,578	38.47	*Clostridiaceae* sp.	77.59	1.72	5	62	1
Bin8	Pre-adapted biomethanation	98	4,897,735	85,849	44.96	*Clostridiales* sp.	–	100%	2	106	2
Bin9	Pre-adapted biomethanation	50	1,655,912	54,434	52.81	Candidatus *Cloacimonetes* sp.	71.25	0	1	58	1
Bin10	Pre-adapted biomethanation	82	1,819,006	33,512	30.41	*Marinilabiliales* sp.	71.24	3.76	1	75	0
Bin11	Anaerobic digestion/Pre-adapted biomethanation	141	1,601,656	17,920	37.99	*Clostridiales* sp.	79.09	0	5	88	1
Bin12	Unadapted biomethanation	109	1,521,905	26,711	49.63	*Clostridiales* sp.	80.88	0	1	96	1

negative effects on the hydrogenotrophic methanogens (Agneessens et al., 2017). However, CH_4 production did not decline during the experimental period in any of the three incubations, suggesting that the methanogenesis remained active throughout the experiment. The methane production rate in the unadapted biomethanation incubations was higher during the 48 hour experimental period, compared to the anaerobic digestion and pre-adapted biomethanation flasks (Fig. 1a). This could potentially be explained by an immediate microbial utilisation of H_2 in the reactor and subsequent increase in methane production rate. Furthermore, the increased H_2 pressure in the biomethanation reactor could also stimulate homoacetogenesis as shown previously (Agneessens et al., 2018), which resulted in a temporary increase in abundance of *Methanosarcinaceae*, which harbour members capable of utilising both H_2 and CO_2, and acetate for methanogenesis. In the present study, the pre-adapted incubations consumed H_2 and CO_2, but did not convert it into methane, which suggests that acetate was produced.

4.2. ^{13}C-bicarbonate protein-SIP

The protein-SIP experiments showed a large number of isotopically enriched peptides in the pre-adapted biomethanation flasks, compared to the anaerobic digestion and unadapted biomethanation incubations (Fig. 2). This is likely related to the prior adaptation of the pre-adapted biomethanation microbiome to the H_2 addition, which could have stimulated the overall activity in the slurry and especially the pathways capable of reducing the added ^{13}C-labelled bicarbonate. This was also reflected in the ^{13}C-labelled MAGs, where 10 of the 12 extracted genomes linked to the ^{13}C-labelled peptides were obtained from the pre-adapted biomethanation bottles. The group of microorganisms capable of utilising CO_2 and H_2 for the production of acetate *via* the WL pathway is taxonomically diverse (Valk et al., 2020), which is also supported by the diverse bacterial taxonomic assignments of the ^{13}C-labelled peptides, which included representatives of *Firmicutes*, *Proteobacteria* and *Bacteroidetes* (Fig. 3). Isotopically enriched peptides deriving from cross-feeding of ^{13}C-labelled CO_2 uptake is considered to be limited due to the relatively short incubation time (48 h), the shallow depth of the proteome and high labelling ratio (RIA).

Furthermore, the functional classification of the detected ^{13}C-labelled peptides with significant incorporation (RIA > 10), belonged mainly to the KEGG categories genetic information processing, carbohydrate metabolism and transport. Previous studies in anaerobic digesters and soil ecosystems using widely utilised substrates such as ^{13}C-labelled acetate, CO_2 and bicarbonate also showed the majority of labelled peptides to belong to essential cell functions and major metabolisms (Li et al., 2019; Mosbaek et al., 2016). In addition, detection of many labelled flagellins and elongation factor Tu is in line with the results of a previous study where protein-SIP was used to detect syntrophic acetate oxidising bacteria (SOAB) in anaerobic digesters using ^{13}C-labelled acetate (Mosbaek et al., 2016).

4.3. Wood-Ljungdahl pathway activity during anaerobic digestion and H_2 biomethanation

In situ biomethanation of hydrogen has previously been suggested to affect the utilisation of the Wood-Ljungdahl pathway, with increased activity having been observed in both directions of the bi-directional conversion, to either biomass or acetate, in previous studies (Agneessens et al., 2017, 2018; Poehlein et al., 2012; Wang et al., 2013). In the present study, isotopic enrichment was also observed for several proteins belonging to the WL pathway, or peripheral downstream metabolisms in all incubation types (Fig. 5). The anaerobic digestion and both the unadapted and pre-adapted biomethanation incubations showed isotopic incorporation in the glycine cleavage system and acetyl-phosphatase, which are present in the periphery of the methyl and carbonyl branch of the WL pathway, respectively. Glycine

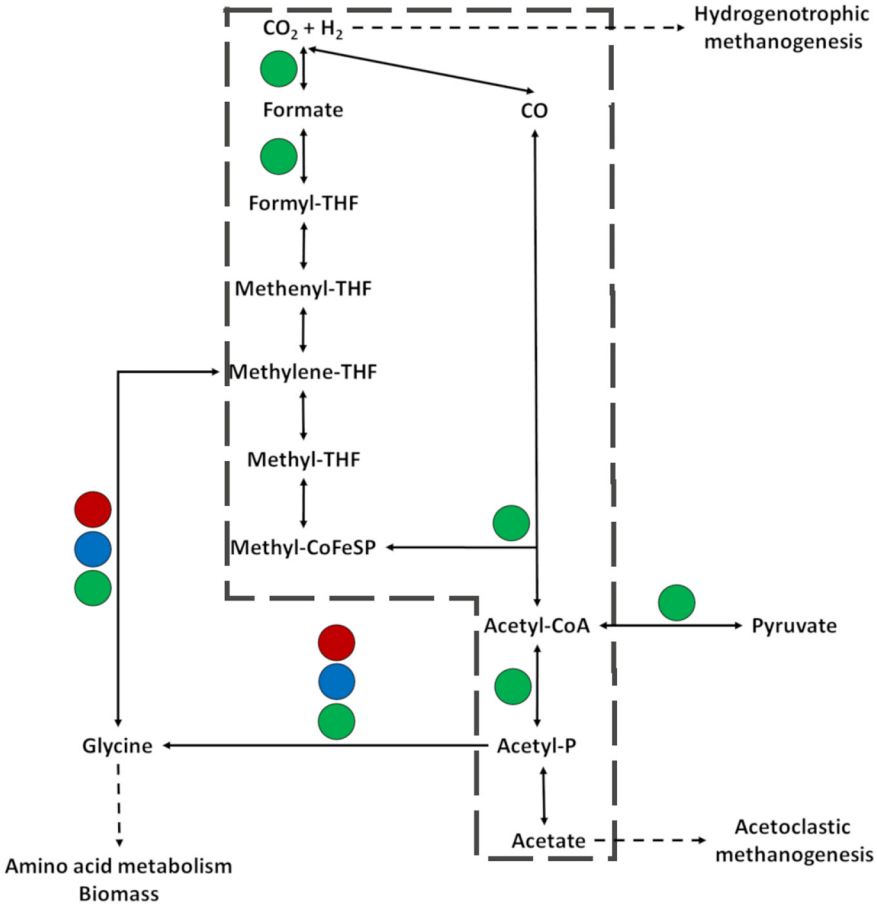

Fig. 5. Overview of the Wood-Ljungdahl pathway and related downstream metabolisms. Detected labelling is indicated with a dot for the respective proteins for the anaerobic digester (red), unadapted biomethanation (blue) and pre-adapted biomethanation (green) incubations. A broken line is drawn around the key genes of the Wood-Ljungdahl pathway.

is a precursor for other amino acids and other complex compounds, and the striking labelling here suggests that a significant amount of the bicarbonate was utilised toward production of biomass. The reductive glycine pathway has been considered an interesting alternative to the Calvin cycle (and the Wood-Ljungdahl pathway) in the biorefinery context (Cotton et al., 2018), and has since also been shown to be naturally occurring as a seventh carbon fixation pathway in *Desulfovibrio desulfuricans* (Sánchez-Andrea et al., 2020).

Furthermore, out of the 12 extracted MAGs (bins) containing matching sequences for the ^{13}C-labelled proteins, only 6 were found to contain the *fhs* gene, the most commonly used biomarker for WL pathway activity, and two bins did not contain evidence of Wood-Ljungdahl utilisation capabilities at all. Moreover, the addition of H_2 in the unadapted biomethanation incubation first led to increased methane production without labelling in the WL pathway to suggest microbial community changes, which suggests that methane was likely produced directly *via* the hydrogenotrophic pathway (Poehlein et al., 2012; Saady, 2013), but this cannot be determined directly as no $^{12}C/^{13}C$ CH_4 measurements were available.

The pre-adapted biomethanation incubations showed ^{13}C-labelled peptides in both the methyl and carbonyl branch of the WL pathway, including the formate-tetrahydrofolate ligase, and the bifunctional carbon monoxide dehydrogenase/acetyl-CoA synthase and phosphotransacetylase. Combined with the observation of the increased H_2 consumption in the pre-adapted biomethanation reactors, it can be suggested that the pre-adapted biomethanation flasks had increased WL pathway activity, and that the ^{13}C-bicarbonate was converted into acetate. This is supported by previous studies that showed that increased H_2 pressure and pH allow homoacetogens to compete more effectively with hydrogenotrophic methanogens (Agneessens et al., 2018; Poehlein et al., 2012; Saady, 2013). It is possible that the consumption of H_2 in the pre-adapted incubations without a net increase in CH_4 formation compared to the AD incubations, stimulated the production of acetate. A fact which is supported by the clear labelling of several steps in WL. Although any produced acetate did not result in additional CH_4 formed, it can have resulted in increased activity (and subsequent labelling) of acetoclastic methanogens *Methanothrix* and *Methanosarcina*, detected in the ^{13}C-labelled peptides from the pre-adapted incubations. It has previously been suggested that strictly acetoclastic methanogens are unaffected by continuous addition of hydrogen, and will be able to convert acetate into methane under *in situ* H_2 biomethanation conditions (Vechi et al., 2021). Alternatively, it is also possible that *Methanosarcina* favoured hydrogen over acetate as its substrate during continuous *in situ* biomethanation as it has previously be shown that acetate metabolism is inhibited by increased H_2 concentration in *M. thermophila* (Ahring et al., 1991).

The results of the present study show good correlation between the process data and the observed isotopic incorporation, especially in the WL pathway, and the method therefore shows promise as a sensitive tool for elucidating further pathways as response to different operational factors during biomethanation. It has also been shown that the origin of the inoculum has a strong effect on the microbiome's ability to adapt to *in situ* H_2 biomethanation (Vechi et al., 2021). Future studies of different inocula and their response to added H_2 could therefore shed further light on the intricate pathways involved when adding exogenous H_2 during biomethanation.

5. Conclusions

The present study showed that H_2 biomethanation stimulated the activity of the microbiome in anaerobic digester systems, and more specifically the expression of genes involved in the Wood-Ljungdahl pathway. Biomass and energy production were the primary fates of the ^{13}C-labelled bicarbonate used to map the metabolic activity in the incubations that were not adapted to hydrogen addition prior to the experiments. The digestate from reactors which had received previous pulses of H_2 showed diverse incorporation of labelled carbon into the microbial community, and in particular organisms containing genes involved in the Wood-Ljungdahl pathway. Here, the strong labelling of key enzymes in the Wood-Ljungdahl pathway corresponded with the fact that the added H_2 did not result in a net increase in formed CH_4, but instead potentially was converted to acetate. A slightly increased pH in these incubations could have been the cause for this response. The use of Protein-SIP using ^{13}C-labelled compounds could prove a strong tool in further elucidating how H_2 and other operational factors impact the different metabolic pathways involved in anaerobic digestion during different operational strategies.

CRediT authorship contribution statement

Nadieh de Jonge: Investigation, Formal analysis, Validation, Data curation, Software, Visualization, Writing – original draft. **Jan Struckmann Poulsen:** Data curation, Software, Writing – original draft. **Nathalia Thygesen Vechi:** Investigation, Methodology. **Michael Vedel Wegener Kofoed:** Conceptualization, Writing – review & editing. **Jeppe Lund Nielsen:** Writing – review & editing, Conceptualization, Methodology, Funding acquisition, Supervision, Validation, Resources.

Declaration of competing interest

The authors declare that they have no known competing financial interests or personal relationships that could have appeared to influence the work reported in this paper.

Acknowledgements

This work was funded by the Novo Nordisk Foundation (Grant no. NNF16OC0021818). The authors wish to thank Henrik Kjeldal and Laura Mia Agneessens for valuable discussions.

Appendix A. Supplementary data

Supplementary data to this article can be found online at https://doi.org/10.1016/j.scitotenv.2021.151254.

References

Agneessens, L.M., Ottosen, L.D.M., Voigt, N.V., Nielsen, J.L., de Jonge, N., Fischer, C.H., Kofoed, M.V.W., 2017. In-situ biogas upgrading with pulse H2 additions: the relevance of methanogen adaption and inorganic carbon level. Bioresour. Technol. 233, 256–263. https://doi.org/10.1016/j.biortech.2017.02.016.

Agneessens, L.M., Ottosen, L.D.M., Andersen, M., Berg Olesen, C., Feilberg, A., Kofoed, M.V.W., 2018. Parameters affecting acetate concentrations during in-situ biological hydrogen methanation. Bioresour. Technol. 258, 33–40. https://doi.org/10.1016/j.biortech.2018.02.102.

Ahring, B.K., Westermann, P., Mah, R.A., 1991. Hydrogen inhibition of acetate metabolism and kinetics of hydrogen consumption by methanosarcina thermophila TM-1. Arch. Microbiol. 157, 38–42. https://doi.org/10.1007/BF00245332.

Albertsen, M., Hugenholtz, P., Skarshewski, A., Nielsen, K.L., Tyson, G.W., Nielsen, P.H., 2013. Genome sequences of rare, uncultured bacteria obtained by differential coverage binning of multiple metagenomes. Nat. Biotechnol. 31, 533–538. https://doi.org/10.1038/nbt.2579.

Angelidaki, I., Treu, L., Tsapekos, P., Kougias, P.G., Campanaro, S., Luo, G., Wenzel, H., 2018. Biogas upgrading and utilization: current status and perspectives. Biotechnol. Adv. 36, 452–466.

Carabeo-Pérez, A., Guerra-Rivera, G., Ramos-Leal, M., Jiménez-Hernández, J., 2019. Metagenomic approaches: effective tools for monitoring the structure and functionality of microbiomes in anaerobic digestion systems. Appl. Microbiol. Biotechnol. 103, 9379–9390. https://doi.org/10.1007/s00253-019-10052-5.

Carballa, M., Regueiro, L., Lema, J.M., 2015. Microbial management of anaerobic digestion: exploiting the microbiome-functionality nexus. Curr. Opin. Biotechnol. 33, 103–111.

Corbellini, V., Kougias, P.G., Treu, L., Bassani, I., Malpei, F., Angelidaki, I., 2018. Hybrid biogas upgrading in a two-stage thermophilic reactor. Energy Convers. Manag. 168, 1–10. https://doi.org/10.1016/j.enconman.2018.04.074.

Cotton, C.A., Edlich-Muth, C., Bar-Even, A., 2018. Reinforcing carbon fixation: CO2 reduction replacing and supporting carboxylation. Curr. Opin. Biotechnol. 49, 49–56. https://doi.org/10.1016/j.copbio.2017.07.014.

de Jonge, N., Moset, V., Møller, H.B., Nielsen, J.L., 2017. Microbial population dynamics in continuous anaerobic digester systems during start up, stable conditions and recovery after starvation. Bioresour. Technol. 232, 313–320. https://doi.org/10.1016/j.biortech.2017.02.036.

de Jonge, N., Davidsson, Å., la Cour Jansen, J., Nielsen, J.L., 2020. Characterisation of microbial communities for improved management of anaerobic digestion of food waste. Waste Manag. 117, 124–135. https://doi.org/10.1016/j.wasman.2020.07.047.

De Vrieze, J., Saunders, A.M., He, Y., Fang, J., Nielsen, P.H., Verstraete, W., Boon, N., 2015. Ammonia and temperature determine potential clustering in the anaerobic digestion microbiome. Water Res. 75, 312–323. https://doi.org/10.1016/j.watres.2015.02.025.

Dupont, C.L., Rusch, D.B., Yooseph, S., Lombardo, M.-J., Alexander Richter, R., Valas, R., Novotny, M., Yee-Greenbaum, J., Selengut, J.D., Haft, D.H., Halpern, A.L., Lasken, R.S., Nealson, K., Friedman, R., Craig Venter, J., 2012. Genomic insights to SAR86, an abundant and uncultivated marine bacterial lineage. ISME J. 6, 1186–1199. https://doi.org/10.1038/ismej.2011.189.

Fotidis, I.A., Karakashev, D., Kotsopoulos, T.A., Martzopoulos, G.G., Angelidaki, I., 2013. Effect of ammonium and acetate on methanogenic pathway and methanogenic community composition. FEMS Microbiol. Ecol. 83, 38–48. https://doi.org/10.1111/j.1574-6941.2012.01456.x.

Fountoulakis, M.S., Petousi, I., Manios, T., 2010. Co-digestion of sewage sludge with glycerol to boost biogas production. Waste Manag. 30, 1849–1853. https://doi.org/10.1016/j.wasman.2010.04.011.

Graf, F., Götz, M., Bajohr, S., 2011. Injection of Biogas, SNG and Hydrogen, pp. 29–40.

Hattori, S., 2008. Syntrophic acetate-oxidizing microbes in methanogenic environments. Microbes Environ. 23, 118–127. https://doi.org/10.1264/jsme2.23.118.

Herbst, F., Bahr, A., Duarte, M., Pieper, D.H., Richnow, H., Bergen, M., Seifert, J., Bombach, P., 2013. Elucidation of in situ polycyclic aromatic hydrocarbon degradation by functional metaproteomics (protein-SIP. Proteomics 13, 2910–2920. https://doi.org/10.1002/pmic.201200569.

Jehmlich, N., Schmidt, F., Taubert, M., Seifert, J., Bastida, F., von Bergen, M., Richnow, H.-H., Vogt, C., 2010. Protein-based stable isotope probing. Nat. Protoc. 5, 1957–1966. https://doi.org/10.1038/nprot.2010.166.

Jensen, M.B., Jensen, B., Ottosen, L.D.M., Kofoed, M.V.W., 2021. Integrating H2 injection and reactor mixing for low-cost H2 gas-liquid mass transfer in full-scale in situ biomethanation. Biochem. Eng. J. 166, 107869. https://doi.org/10.1016/j.bej.2020.107869.

Lecker, B., Illi, L., Lemmer, A., Oechsner, H., 2017. Biological hydrogen methanation – a review. Bioresour. Technol. 245, 1220–1228. https://doi.org/10.1016/j.biortech.2017.08.176.

Li, Z., Yao, Q., Guo, X., Crits-Christoph, A., Mayes, M.A., IV, W.J.H., Lebeis, S.L., Banfield, J.F., Hurst, G.B., Hettich, R.L., Pan, C., 2019. Genome-resolved proteomic stable isotope probing of soil microbial communities using 13CO2 and 13C-methanol. Front. Microbiol. 10, 1–14. https://doi.org/10.3389/fmicb.2019.02706.

Luo, G., Johansson, S., Boe, K., Xie, L., Zhou, Q., Angelidaki, I., 2012. Simultaneous hydrogen utilization and in situ biogas upgrading in an anaerobic reactor. Biotechnol. Bioeng. 109, 1088–1094. https://doi.org/10.1002/bit.24360.

Menzel, P., Ng, K.L., Krogh, A., 2016. Fast and sensitive taxonomic classification for metagenomics with kaiju. Nat. Commun. 7, 11257. https://doi.org/10.1038/ncomms11257.

Mosbaek, F., Kjeldal, H., Mulat, D.G., Albertsen, M., Ward, A.J., Feilberg, A., Nielsen, J.L., 2016. Identification of syntrophic acetate-oxidizing bacteria in anaerobic digesters by combined protein-based stable isotope probing and metagenomics. ISME J. 10, 2405–2418.

Mulat, D.G., Mosbæk, F., Ward, A.J., Polag, D., Greule, M., Keppler, F., Nielsen, J.L., Feilberg, A., 2017. Exogenous addition of H2 for an in situ biogas upgrading through biological reduction of carbon dioxide into methane. Waste Manag. 68, 146–156. https://doi.org/10.1016/J.WASMAN.2017.05.054.

Narihiro, T., Nobu, M.K., Kim, N.K., Kamagata, Y., Liu, W.T., 2015. The nexus of syntrophy-associated microbiota in anaerobic digestion revealed by long-term enrichment and community survey. Environ. Microbiol. 17, 1707–1720. https://doi.org/10.1111/1462-2920.12616.

Nizami, A.-S., 2012. Anaerobic digestion: processes, products, and applications. In: Caruana, D.J., Olsen, A.E. (Eds.), Anaerobic Digestion: Processes, Products, and Applications. Nova Science Publishers, Inc, New York, NY, p. 16.

Parks, D.H., Imelfort, M., Skennerton, C.T., Hugenholtz, P., Tyson, G.W., 2015. CheckM: assessing the quality of microbial genomes recovered from isolates, single cells, and metagenomes. Genome Res. 25, 1043–1055. https://doi.org/10.1101/gr.186072.114.

Peydaei, A., Bagheri, H., Gurevich, L., de Jonge, N., Nielsen, J.L., 2020. Impact of polyethylene on salivary glands proteome in galleria melonella. Comp. Biochem. Physiol. Part D Genomics Proteomics, 100678. https://doi.org/10.1016/j.cbd.2020.100678.

Poehlein, A., Schmidt, S., Kaster, A.-K., Goenrich, M., Vollmers, J., Thürmer, A., Bertsch, J., Schuchmann, K., Voigt, B., Hecker, M., Daniel, R., Thauer, R.K., Gottschalk, G., Müller, V., 2012. An ancient pathway combining carbon dioxide fixation with the generation and utilization of a sodium ion gradient for ATP synthesis. PLoS One 7, e33439.

R Development Core Team, 2021. R: A Language and Environment for Statistical Computing. R Foundation for Statistical Computing, Vienna, Austria.

Saady, N.M.C., 2013. Homoacetogenesis during hydrogen production by mixed cultures dark fermentation: unresolved challenge. Int. J. Hydrog. Energy 38, 13172–13191. https://doi.org/10.1016/j.ijhydene.2013.07.122.

Sachsenberg, T., Herbst, F.A., Taubert, M., Kermer, R., Jehmlich, N., Von Bergen, M., Seifert, J., Kohlbacher, O., 2015. MetaProSIP: automated inference of stable isotope incorporation rates in proteins for functional metaproteomics. J. Proteome Res. 14, 619–627. https://doi.org/10.1021/pr500245w.

Sánchez-Andrea, I., Guedes, I.A., Hornung, B., Boeren, S., Lawson, C.E., Sousa, D.Z., Bar-Even, A., Claassens, N.J., Stams, A.J.M., 2020. The reductive glycine pathway allows autotrophic growth of Desulfovibrio desulfuricans. Nat. Commun. 11, 1–12. https://doi.org/10.1038/s41467-020-18906-7.

Sawatdeenarunat, C., Nguyen, D., Surendra, K.C., Shrestha, S., Rajendran, K., Oechsner, H., Xie, L., Khanal, S.K., 2016. Anaerobic biorefinery: current status, challenges, and opportunities. Bioresour. Technol. 215, 304–313. https://doi.org/10.1016/j.biortech.2016.03.074.

Seemann, T., 2014. Prokka: rapid prokaryotic genome annotation. Bioinformatics 30, 2068–2069. https://doi.org/10.1093/bioinformatics/btu153.

Treu, L., Campanaro, S., Kougias, P.G., Sartori, C., Bassani, I., Angelidaki, I., 2018. Hydrogen-fueled microbial pathways in biogas upgrading systems revealed by genome-centric metagenomics. Front. Microbiol. 9, 1–16 (1079).

Valk, L.C., Diender, M., Stouten, G.R., Petersen, J.F., Nielsen, P.H., Dueholm, M.S., Pronk, J.T., van Loosdrecht, M.C.M., 2020. "Candidatus galacturonibacter soehngenii" shows acetogenic catabolism of galacturonic acid but lacks a canonical carbon monoxide Dehydrogenase/Acetyl-CoA synthase complex. Front. Microbiol. 11, 1–12. https://doi.org/10.3389/fmicb.2020.00063.

Vanwonterghem, I., Jensen, P.D., Ho, D.P., Batstone, D.J., Tyson, G.W., 2014. Linking microbial community structure, interactions and function in anaerobic digesters using new molecular techniques. Curr. Opin. Biotechnol. 27, 55–64. https://doi.org/10.1016/j.copbio.2013.11.004.

Vechi, N.T., Agneessens, L.M., Feilberg, A., Ottosen, L.D.M., Kofoed, M.V.W., 2021. In situ biomethanation: inoculum origin influences acetate consumption rate during hydrogen addition. Bioresour. Technol. Rep. 14, 100656. https://doi.org/10.1016/j.biteb.2021.100656.

Wahid, R., Mulat, D.G., Gaby, J.C., Horn, S.J., 2019. Effects of H2:CO2 ratio and H2 supply fluctuation on methane content and microbial community composition during in-situ biological biogas upgrading. Biotechnol. Biofuels 12, 104. https://doi.org/10.1186/s13068-019-1443-6.

Wang, W., Xie, L., Luo, G., Zhou, Q., Angelidaki, I., 2013. Performance and microbial community analysis of the anaerobic reactor with coke oven gas biomethanation and in situ biogas upgrading. Bioresour. Technol. 146, 234–239. https://doi.org/10.1016/j.biortech.2013.07.049.

Ward, A.J., Hobbs, P.J., Holliman, P.J., Jones, D.L., 2008. Optimisation of the anaerobic digestion of agricultural resources. Bioresour. Technol. 99, 7928–7940. https://doi.org/10.1016/j.biortech.2008.02.044.

Weiland, P., 2010. Biogas production: current state and perspectives. Appl. Microbiol. Biotechnol. 85, 849–860. https://doi.org/10.1007/s00253-009-2246-7.

Wickham, H., 2016. ggplot2: Elegant Graphics for Data Analysis. Springer-Verlag, New York.